

# Hydrated HCl Clusters, $\text{HCl}(\text{H}_2\text{O})_{1-3}$ , in Helium Nanodroplets: Studies of Free OH Vibrational Stretching Modes<sup>†</sup>

Dmitry Skvortsov,<sup>‡</sup> Seung Jun Lee,<sup>§</sup> Myong Yong Choi,<sup>\*,§</sup> and Andrey F. Vilesov<sup>\*,‡</sup>

Department of Chemistry, University of Southern California, Los Angeles, California 90089, and Department of Chemistry and Research Institute of Natural Sciences, Gyeongsang National University, Jinju 660-701, South Korea

Received: December 30, 2008; Revised Manuscript Received: February 26, 2009

In this work, infrared laser spectroscopy in helium droplets is used to study the solvation of HCl with small water clusters. Clusters of  $\text{HCl}(\text{H}_2\text{O})_n$  with  $n = 1-3$  and  $(\text{HCl})_2\text{H}_2\text{O}$  have been identified in the free OH stretching spectral range of  $3680-3820\text{ cm}^{-1}$ . The assignment of the infrared vibrational bands of the clusters is aided by ab initio calculations.

## 1. Introduction

Because of its fundamental significance in chemistry, the microscopic mechanism of ionization of acid molecules in solvents such as water has attracted considerable attention. HCl molecules solvated in small water clusters have long been considered as a model system. Solvation and ionization of HCl molecules in water clusters has been extensively studied via theoretical calculations.<sup>1-7</sup> It was found that  $\text{HCl}(\text{H}_2\text{O})_n$  ( $n = 1-3$ ) clusters have hydrogen-bonded cyclic structures.<sup>1</sup> Calculations<sup>1-6,8</sup> have also shown that the length of the H–Cl bond increases with  $n$  and HCl eventually dissociates in clusters having four and larger number of water molecules. Thus, tetramers already show the formation of  $\text{H}_3\text{O}^+$  and  $\text{Cl}^-$  ions, characteristic of aqueous acid solutions. Anharmonic vibrational calculations for  $(\text{HCl})_n(\text{NH}_3)_n$  and  $(\text{HCl})_m(\text{H}_2\text{O})_m$  mixed clusters by Gerber and co-workers<sup>9</sup> have shown that ionization takes place at  $n = 2$  and  $m = 4$ , respectively. A number of molecular dynamics and Monte Carlo simulations of proton transfer in aqueous HCl solutions and on the surface of ice crystals have also been reported.<sup>3,7,8,10,11</sup>

Experimental study of  $\text{HCl}(\text{H}_2\text{O})_n$  clusters has proven to be challenging. Spectroscopy in low temperature solid matrices has been extensively used to search for the zwitterionic form of  $\text{HCl}(\text{H}_2\text{O})_n$  clusters<sup>12-14</sup> as well as in clusters of HCl and  $\text{NH}_3$  molecules.<sup>15,16</sup> However, the large width of the spectral bands due to the strong interaction with the matrix material as well as poor control over cluster composition have contributed to the ambiguity in assignment of the spectra of clusters larger than dimers. Devlin and co-workers have reported FT-IR spectra of HCl molecules adsorbed on nanocrystalline ice films.<sup>10,17-19</sup> Using the results of the Monte Carlo and ab initio calculations, the observed spectra were assigned to the molecular and ionized HCl molecules depending on the temperature and the HCl coverage of the ice films.<sup>7,10</sup> The spectra of free  $\text{HCl}-\text{H}_2\text{O}$  complexes obtained with “ragout-jet” using FT-IR absorption spectroscopy<sup>20,21</sup> showed a broadband ( $\Delta\nu \approx 200\text{ cm}^{-1}$ ) around  $2570\text{ cm}^{-1}$ , which is close to the calculated vibrational frequency of the  $\text{H}_3\text{O}^+\cdots\text{Cl}^-$  ion pairs. The broadband was later assigned to molecular HCl on the basis of the results of the ragout-jet

and ice nanocrystal experiments, which involve substitution by  $\text{D}_2\text{O}$  and measurements at different temperatures, respectively.<sup>17</sup> The assignment of the gas-phase spectra is complicated due to the large breadth of the bands along with unknown size distribution and molecular composition of the clusters obtained in the free jet expansion.  $\text{HCl}-\text{H}_2\text{O}$  binary complexes as well as their deuterated analogues were also studied in molecular beams via high-resolution infrared cavity ringdown spectroscopy by Saykally and co-workers.<sup>22</sup> Finally, it is worthwhile to note a related study of HBr dissociation in small water clusters by Hurley et al., which had employed a femtosecond pump–probe technique.<sup>23,24</sup> The authors concluded that the complete dissociation of HBr takes place in clusters having five water molecules based on the absence of the signal due to  $\text{H}^+(\text{H}_2\text{O})_5$  ions. However, the technique does not provide information on the structure of the clusters that could be derived from the infrared spectra.

In this work, we report on the infrared spectroscopic study of clusters of HCl with up to three water molecules, which have been assembled in helium droplets and probed via infrared depletion spectroscopy in the range of free OH stretching modes of the clusters. This range is especially difficult in the gas phase and in matrix isolation techniques due to small splitting of the bands of different complexes and severe overlap with bands from water clusters. The assignment of the infrared vibrational bands of the clusters is supported by the ab initio calculations.

## 2. Experimental Method and ab Initio Calculations

**2.1. Experiments.** Helium droplets provide the ultimate matrix for formation and high resolution spectroscopy of molecular clusters.<sup>25-28</sup> The superfluid state of the droplets contributes to the observation of free molecular rotation and extremely narrow ro-vibrational spectral lines in He droplets.<sup>26,29,30</sup> The helium nanodroplet technique has been described in detail elsewhere.<sup>25-28</sup> In this work, helium nanodroplets having an average size of about 4000 atoms are formed during supersonic expansion of high purity helium (99.9999%) gas at  $P_0 = 20$  bar into vacuum through a  $5\text{ }\mu\text{m}$  nozzle at a temperature of  $T_0 = 16\text{ K}$ . The droplets capture HCl first and then  $\text{H}_2\text{O}$  molecules in the two consecutive pick-up chambers arranged along the droplet beam. Upon pickup, molecules recombine rapidly to form clusters. Infrared spectra of the clusters were obtained using a pulsed optical parametric oscillator/amplifier (LaserVision, 7 ns duration, 20 Hz repetition rate, 1 mJ pulse energy) having a

<sup>†</sup> Part of the “Robert Benny Gerber Festschrift”.

\* Corresponding author. Tel.: +82-55-751-6017. Fax: +82-55-761-0244. E-mail: mychoi@gnu.kr (M.Y.C.); vilesov@usc.edu (A.F.V.).

<sup>‡</sup> University of Southern California.

<sup>§</sup> Gyeongsang National University.

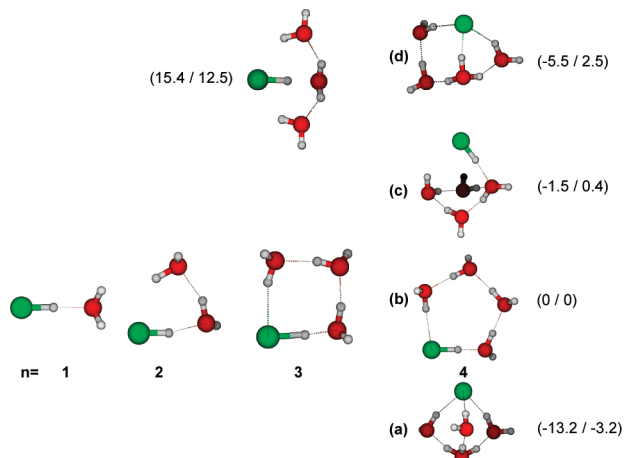


**Figure 1.** The optimized structures of  $\text{HCl}(\text{H}_2\text{O})_n$  complexes, calculated at the MP2 level with an aug-cc-pVDZ basis set using Gaussian 03. The four most stable isomers of the complexes with four water molecules are shown on the right in order of increasing binding energy. The binding energy of the cyclic isomer (b) is set to zero. The values in the brackets are energies in kJ/mol without/with a harmonic zero-point energy correction.

line width of 0.1 or  $1\text{ cm}^{-1}$  with injection seeding of the pump laser on or off, respectively. The laser cabinet and the optical pathways were purged with dry nitrogen continuously to prevent absorption from water in the air. The laser beam was aligned antiparallel and coaxial to the helium nanodroplet beam. The absorption of laser photons by encapsulated clusters is followed by rapid energy transfer to the host He droplets and subsequent evaporation of several hundreds of helium atoms. The total flux of the droplet beam is detected by a quadrupole mass filter, which is adjusted to transmit all masses larger than 6 u. The absorption leads to a transient decrease of the mass spectrometer signal, which is recorded by a lock-in amplifier.

**2.2. Ab Initio Calculations.** To review the trends in the spectra upon increase of the cluster size at the same level of theory, we carried out systematic calculations of the structure, energetics, and infrared spectra of the  $\text{HCl}(\text{H}_2\text{O})_n$  clusters using the Møller–Plesset perturbation theory at the second-order (MP2) level. The geometries of all molecules have been fully optimized with the Dunning’s correlation consistent polarized valence double- $\zeta$  basis set augmented with diffuse functions (aug-cc-pVDZ) basis set using Gaussian 03.<sup>31</sup> The optimized structures have no negative vibrational frequencies showing the local minima of the potential energy surface. The structures of the  $\text{HCl}(\text{H}_2\text{O})_n$  complexes are shown in Figure 1, which are in agreement with the results of the previous calculations.<sup>1–6</sup> In the complexes having up to three water molecules, the global minimum corresponds to the cyclic hydrogen-bonded clusters. For the  $\text{HCl}(\text{H}_2\text{O})_4$  clusters, several noncyclic isomers were identified.

The calculations confirm the importance of the zero-point energy (ZPE) contribution to the total energy. Without taking into account ZPE, the cyclic isomer of  $\text{HCl}(\text{H}_2\text{O})_4$  has the highest energy among the complexes. However, with the ZPE contribution, it becomes the second most stable isomer, in agreement with previous calculations.<sup>2,4</sup> Considering the close energies (within 6 kJ/mol) of all four isomers of  $\text{HCl}(\text{H}_2\text{O})_4$  in Figure 1, we expect that the vibration along the configurational coordinates connecting different isomers will be highly anharmonic, which is not taken into account in the calculations. Therefore, the relative stability of the different hydrogen bonding and zwitterionic isomers is probably beyond the quality of the present calculations and awaits experimental verification.

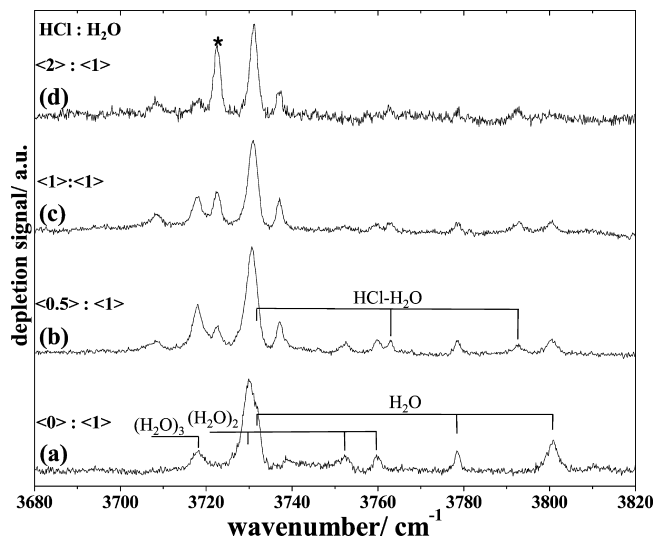


**Figure 2.** Spectra of  $(\text{HCl})_m(\text{H}_2\text{O})_n$  clusters measured at different abundance of HCl molecules  $\langle m \rangle$  as shown in each panel and at constant  $\langle N_{\text{water}} \rangle = 1$ .

For each of the structures in Figure 1, harmonic vibrational frequencies and corresponding infrared intensities have been calculated. The calculated and measured spectra will be compared later.

### 3. Experimental Results

From previous work,<sup>25–28</sup> it is known that the average number of the molecules captured by He droplets is proportional to the pickup pressure. To obtain the proportionality coefficients, we have measured the pickup pressure dependencies of the intensity of the bands of single  $\text{H}_2\text{O}$  or  $\text{HCl}$  molecule, which reach their maxima upon average capture of single molecule per droplet. The measured Poisson dependencies at similar experimental conditions have been published previously in ref 32 and in the Supporting Information of ref 33. In the following, the average numbers of the captured molecules are shown in brackets; for example,  $\langle 1 \rangle : \langle 2 \rangle$  corresponds to formation of the clusters having on average one  $\text{HCl}$  and two water molecules. The probability of formation of clusters of a particular composition is given by the Poisson distribution.<sup>34</sup>

**3.1. Spectra of the  $\text{HCl}(\text{H}_2\text{O})_n$  Clusters.** Figure 2 shows the spectra of the  $\text{HCl}(\text{H}_2\text{O})_n$  clusters as measured at increasing abundance of  $\text{HCl}$  and at constant  $\text{H}_2\text{O}$  content of  $\langle N_{\text{water}} \rangle = 1$ . Similar spectra obtained at  $\langle N_{\text{water}} \rangle = 0.5$  are shown in Figure S1 in the Supporting Information. Spectrum (a) obtained in the absence of the  $\text{HCl}$  molecules shows ro-vibrational lines of the asymmetric stretch of  $\text{H}_2\text{O}$  monomers as well as free OH stretching bands in dimers and trimers (Table 1).<sup>35</sup> At  $\langle N_{\text{water}} \rangle = 1$ , the band of  $\text{H}_2\text{O}$  trimer at  $3718\text{ cm}^{-1}$  is weak, in agreement with small abundance of the trimers in the droplets. Upon admission of the  $\text{HCl}$  molecules, several new peaks appear in the spectra (b)–(d), which must be due to clusters of  $\text{HCl}$  with one or two water molecules. The peaks in the range of  $3730\text{--}3800\text{ cm}^{-1}$  are assigned to binary  $\text{HCl}\text{--}\text{H}_2\text{O}$  complexes, based on the linear increase of their intensities with respect to the water monomer lines. Because the relative intensities of the peaks at  $3708$  and  $3718\text{ cm}^{-1}$  with respect to the  $\text{HCl}\text{--}\text{H}_2\text{O}$  lines in Figure 2b–d remain the same upon increase of  $\langle N_{\text{HCl}} \rangle$ , these bands were assigned to the clusters having single  $\text{HCl}$  molecule. In the spectrum of Figure 2a, the peak at  $3730\text{ cm}^{-1}$  stems from the unresolved free OH stretching band of  $\text{H}_2\text{O}$  donor molecules in the water dimer and the P(1) line in the

TABLE 1: Identified Free O–H Stretching Bands in (HCl)<sub>m</sub>(H<sub>2</sub>O)<sub>n</sub> Clusters

(HCl) <sub>m</sub> (H <sub>2</sub> O) <sub>n</sub>								
<i>m</i> : <i>n</i>	frequency	assignment	<i>m</i> : <i>n</i>	frequency	assignment	<i>m</i> : <i>n</i>	frequency	assignment
0:1	3800.94	R(1)	1:1	3792.6	R(1)	2:1	3722.6	OH (F)
	3778.23	R(0)		3762.9	R(0)			
	3731.95	P(1)		3732.2 <sup>a</sup>	P(1)			
				3737	<sup>b</sup>			
0:2	3753	OH (AS) acceptor	1:2	3731	OH (F)	2:2	3731	OH (F)
	3760.0	OH (AS) acceptor		3708	OH (F)			
	3730	OH (F) donor						
	3654	OH(SS) acceptor						
0:3	3718.1	OH (F)	1:3	3718	OH (F)	2:3	3718	OH (F)
				3708	OH (F) acceptor		3708	OH (F) acceptor

<sup>a</sup> Not resolved due to the overlap of the high frequency shoulder of the water dimer band at around 3730 cm<sup>-1</sup>. <sup>b</sup> Unassigned.

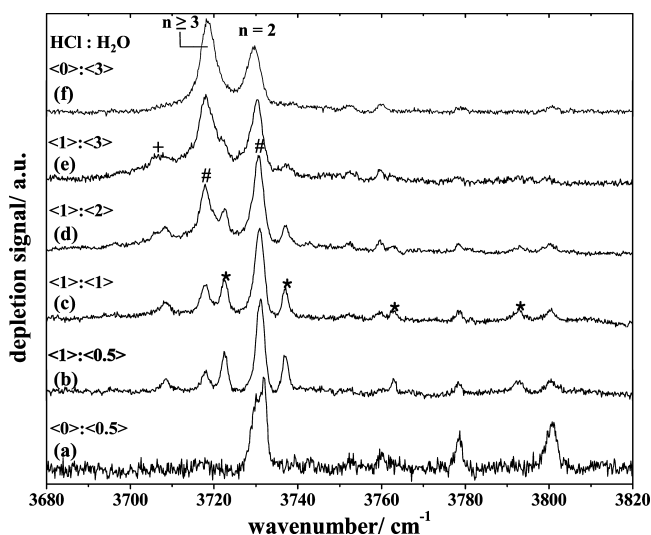


**Figure 3.** Spectra of (HCl)<sub>m</sub>(H<sub>2</sub>O)<sub>n</sub> clusters measured at different abundance of H<sub>2</sub>O molecules ( $\langle n \rangle = 0.5$ –3) as shown in each panel and at constant  $\langle N_{\text{HCl}} \rangle = 1$ , traces (b)–(e). Traces (a) and (f) are reference spectra obtained at  $\langle N_{\text{water}} \rangle = 0.5$  and 3, respectively, without HCl added.

single water molecule.<sup>35</sup> The intensity of the spectral features due to water monomers and dimers decreases upon introduction of the HCl, whereas the peak at 3730 cm<sup>-1</sup> remains strong in Figure 2d upon average capture of two HCl molecules. Therefore, we concluded that this peak has a large contribution from the OH bands of the HCl(H<sub>2</sub>O)<sub>2</sub> or (HCl)<sub>2</sub>(H<sub>2</sub>O)<sub>2</sub> clusters. Finally, the intensity of the band at 3723 cm<sup>-1</sup> asterisked in Figure 2d increases as a square of  $\langle N_{\text{HCl}} \rangle$ . It must therefore be assigned to clusters having predominantly two HCl molecules.

Figure 3 shows the spectra obtained at constant  $\langle N_{\text{HCl}} \rangle = 1$  and at different abundance of water molecules. Similar spectra obtained at  $\langle N_{\text{HCl}} \rangle = 0.5$  are shown in the Supporting Information (see Figure S2). For comparison, Figure 3a and f shows the spectra obtained in the absence of HCl at  $\langle N_{\text{water}} \rangle = 0.5$  and 3, respectively. The strong bands at 3730 and 3718 cm<sup>-1</sup> in Figure 3f are due to the free OH stretches in neat water clusters having  $n = 2$  and  $n \geq 3$  molecules, respectively.<sup>35</sup> Additional peaks in spectra (b)–(e) measured with HCl added are marked with asterisks. Because the relative intensity of the additional peaks remains constant upon increase of the  $\langle N_{\text{water}} \rangle$ , we concluded that they stem from clusters of HCl with single H<sub>2</sub>O molecules. Upon increase of  $\langle N_{\text{water}} \rangle$ , the features due to (HCl)<sub>m</sub>(H<sub>2</sub>O)<sub>n</sub> clusters fade out. The spectrum (e) measured for HCl with the highest abundance of water in clusters is very similar to that in

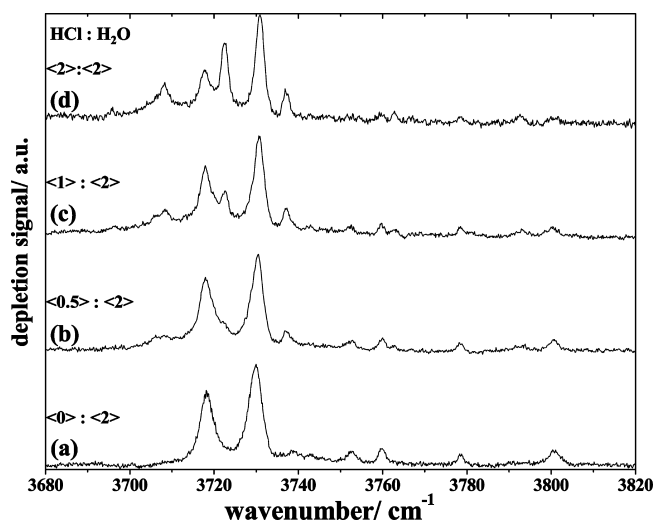


**Figure 4.** Same as in Figure 2 but with  $\langle N_{\text{water}} \rangle = 2$ .

neat water clusters (f), with the notable exception of a broad weak band at around 3707 cm<sup>-1</sup> marked with a “+”.

Figure 4 shows the  $\langle N_{\text{HCl}} \rangle$  dependence of the spectra obtained at larger constant  $\langle N_{\text{water}} \rangle = 2$ . Besides the spectral features already discussed earlier, the most noticeable change in the spectra upon addition of HCl occurred in the range of 3700–3740 cm<sup>-1</sup>. The band at around 3730 cm<sup>-1</sup> in the spectrum (a) originates from the free OH stretch vibration in the donor molecule of water dimers. Upon increase of the  $\langle N_{\text{HCl}} \rangle$ , the band gets narrower and its frequency is blue-shifted by about 1 cm<sup>-1</sup>, while its relative intensity as compared to that in the neat water spectrum (a) remains almost unchanged. According to Poisson distribution, the abundance of neat (H<sub>2</sub>O)<sub>2</sub> in the droplets upon additional capture of average two HCl molecules as in spectrum (d) should be about 14%. Therefore, the band at 3731 cm<sup>-1</sup> in Figure 4d must have dominant contributions from HCl(H<sub>2</sub>O)<sub>2</sub>, (HCl)<sub>2</sub>(H<sub>2</sub>O)<sub>2</sub>, and (HCl)<sub>3</sub>(H<sub>2</sub>O)<sub>2</sub> clusters, and thus the frequency of their free OH stretches should be the same as in water dimers within  $\pm 2$  cm<sup>-1</sup>. The band at 3718 cm<sup>-1</sup> in Figure 4a comes predominantly from H<sub>2</sub>O trimers with about 30% contribution from water tetramers. Upon increase of  $\langle N_{\text{HCl}} \rangle$ , the relative intensity of the band at 3718 cm<sup>-1</sup> decreases, and new bands at 3708 and 3696 cm<sup>-1</sup> appear. At highest  $\langle N_{\text{HCl}} \rangle = 2$ , in Figure 4d the intensities of the bands at 3708 and 3718 cm<sup>-1</sup> are comparable. We assigned these bands to the clusters of water trimers and tetramers with up to three HCl molecules. As references, the survey spectra of neat water clusters obtained at different number of H<sub>2</sub>O molecules in the range of  $\langle N_{\text{water}} \rangle = 0.5$ –3 are shown in Figure S3 in the Supporting Information.



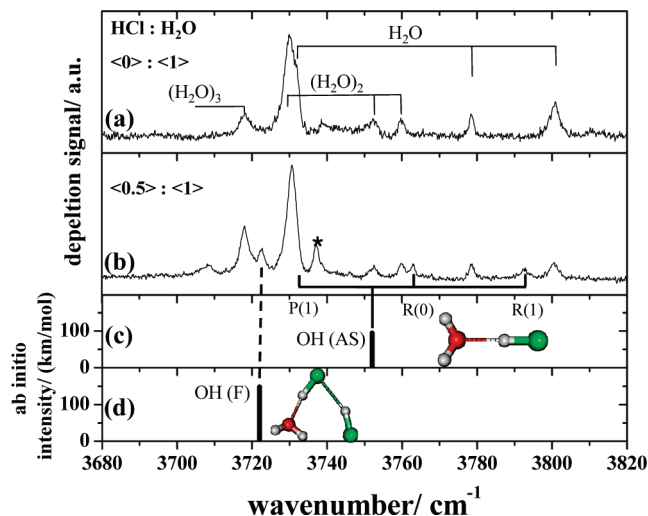


**Figure 5.** Spectrum of  $\text{H}_2\text{O}$  clusters at  $\langle N_{\text{water}} \rangle = 1$  (a) and  $(\text{HCl})_m(\text{H}_2\text{O})_n$  clusters obtained upon addition of HCl to  $\langle N_{\text{HCl}} \rangle = 0.5$  (b). The band marked with an asterisk is discussed in the text. The calculated spectra of the  $\text{HCl}-\text{H}_2\text{O}$  and  $(\text{HCl})_2\text{H}_2\text{O}$  clusters are shown in panels (c) and (d), respectively. The lines show the assignments of the bands. The calculated frequencies are scaled by a factor of 0.957.

## 4. Discussion

**4.1.  $\text{HCl}-\text{H}_2\text{O}$  Clusters.**  $\text{HCl}-\text{H}_2\text{O}$  clusters and their isotopologues have been extensively studied in the gas phase via microwave spectroscopy,<sup>36,37</sup> and infrared spectroscopy in the range of H–Cl vibrations<sup>20,22</sup> as well as via matrix isolation spectroscopy.<sup>12,14,38</sup> According to ref 39, the equilibrium configuration of the complex is bent with the angle between the  $C_{2v}$  axis of the water molecules and the  $\text{O}\cdots\text{H}$  hydrogen bond of  $\varphi = 46^\circ$ . The complex has two equivalent minima at  $\pm\varphi$  separated by a potential barrier of  $80\text{ cm}^{-1}$ . The zero-point vibrational level of the complex lies about  $10\text{ cm}^{-1}$  below the barrier, whereas the first excited vibrational level is about  $60\text{ cm}^{-1}$  higher than the ground state. Therefore, the ground state of the complex is delocalized over the two minima, and the complex has an effective  $C_{2v}$  symmetry. The expectation value of the angle has been calculated to be  $\langle\varphi\rangle = 35^\circ$ , from which the principal rotational constant of the complex can be estimated to be  $A = 12\text{ cm}^{-1}$ . The complex is a nearly prolate symmetric top with  $B \approx C \approx 0.013\text{ cm}^{-1}$ .<sup>39</sup> On the other hand, a rotational constant for the  $\text{HCl}-\text{H}_2\text{O}$  complex of  $A = 14\text{--}15\text{ cm}^{-1}$  has been recently estimated from the FT-IR spectra in free jet.<sup>20</sup> Such a high value of the  $A$  constant corresponds to the  $C_{2v}$  structure of the complex with the  $C_2$  axis of water molecule nearly coaxial with the HCl axis. Previous studies<sup>25–27</sup> indicated that the rotational constants of light rotors ( $B_{\text{gas}} > 1\text{ cm}^{-1}$ ) in helium are only a few percent smaller than those in the gas phase, justifying their direct comparison.

Figure 5 shows the comparison of the measured spectrum of water molecules and clusters at  $\langle N_{\text{water}} \rangle = 1$  (a) and that upon addition of HCl to  $\langle N_{\text{HCl}} \rangle = 0.5$  (b). The peaks at  $3762.9$  and  $3792.6\text{ cm}^{-1}$  were assigned to the  $R(0)$  and  $R(1)$  lines of free OH asymmetric stretching mode ( $\nu_3$ ) of water molecules in the  $\text{HCl}-\text{H}_2\text{O}$  binary complexes. The  $K = 1$  state of the complex remains populated at  $T = 0.38\text{ K}$  in the droplets because it originates from *ortho*- $\text{H}_2\text{O}$  molecules having nuclear spin of  $I = 1$ , which remains unrelaxed in the droplets, similar to that in single water molecules.<sup>35</sup> The end-over-end rotational structure remains unresolved due to the small value of the rotational constants  $B$  and  $C$  in free complexes. The band of the  $\text{HCl}-\text{H}_2\text{O}$

complexes corresponds to excitation of the asymmetric stretch of water, and this is a perpendicular band. Therefore, the frequency gap between the  $R(K = 0)$  at  $3762.9\text{ cm}^{-1}$  and  $R(K = 1)$  at  $3792.6\text{ cm}^{-1}$  sub-bands of about  $29.7\text{ cm}^{-1}$  allows one to obtain the  $A$  rotational constant in the complex as  $14.85\text{ cm}^{-1}$ , which is larger than that estimated from the results of ref 39. This may indicate that the liquid helium environment constrains the large amplitude ( $\pm 0.4\text{ \AA}$ ) motion of the H atoms in the double well potential. If this interpretation is correct, this would place the  $P(1)$  line of  $\text{HCl}-\text{H}_2\text{O}$  at  $3733.2\text{ cm}^{-1}$ , which cannot be resolved due to the overlap with the high frequency shoulder of the water dimer band at around  $3730\text{ cm}^{-1}$ . According to this assignment, the origin of the  $\nu_3$  band of  $\text{HCl}-\text{H}_2\text{O}$  should be at  $3748.0\text{ cm}^{-1}$ , which is close to the  $\nu_3$  band origin in single  $\text{H}_2\text{O}$  molecules in He droplets at  $3755.1\text{ cm}^{-1}$ .<sup>35</sup> This is also close to the calculated frequency of the asymmetric OH stretches, which are shown in Figure 5c. In this work, the ab initio frequencies were scaled by a factor of 0.957.

There is an important point of disconcert to this picture. According to the pickup pressure dependences, the band at  $3737.2\text{ cm}^{-1}$  marked with an asterisk in Figure 5b has also been assigned to  $\text{HCl}-\text{H}_2\text{O}$  binary complexes; however, its origin is difficult to explain. This is certainly not the  $P(1)$  line of the  $\nu_3$  band; this would require that its intensity be weaker than that of the  $R(1)$  line, which is not the case. We have considered assigning the band at  $3737.2\text{ cm}^{-1}$  to some other isomer of the  $\text{HCl}-\text{H}_2\text{O}$  complexes, in which, for example, water can play the role of the donor molecule. However, such complexes must have an HCl stretching frequency close to that in free HCl molecules, which has not been observed.<sup>40</sup> Moreover, ab initio calculations in this work did not give a stable minimum for the complex in which water molecule serves as a donor. Therefore, the assignment of the band at  $3737.2\text{ cm}^{-1}$  remains uncertain at the moment.

**4.2.  $(\text{HCl})_2\text{H}_2\text{O}$  Clusters.** Based on the pickup pressure dependences as discussed earlier, the band at  $3722.6\text{ cm}^{-1}$  is attributed to the free OH stretching mode in  $(\text{HCl})_2\text{H}_2\text{O}$  clusters. Its frequency matches the calculated one when the result of MP2/aug-cc-pVDZ calculations is scaled by a factor of 0.957, as shown in Figure 5d. Trimers and larger clusters have calculated rotational constants of less than  $0.1\text{ cm}^{-1}$ . Therefore, the rotational structure in the bands of trimers and larger clusters cannot be resolved. The maxima of the spectral peaks should therefore give the position of the band origins of the corresponding vibrational bands.

**4.3.  $\text{HCl}(\text{H}_2\text{O})_2$  Clusters.** We now move on to the assignments of the bands of clusters having more than one water molecule. Figure 6 shows the comparison of the spectra measured at  $\langle N_{\text{water}} \rangle = 0.5$  (a) and  $\langle N_{\text{HCl}} \rangle : \langle N_{\text{water}} \rangle = 1:0.5$  (b). The two asterisked bands at  $3708$  and  $3731\text{ cm}^{-1}$  likely originated from the  $\text{HCl}(\text{H}_2\text{O})_2$  clusters. The band marked with a “#” is assigned to the  $(\text{HCl})_2\text{H}_2\text{O}$  cluster. Panel (c) shows the calculated spectrum of the pseudocyclic  $\text{HCl}(\text{H}_2\text{O})_2$  clusters. It is seen that the scaled calculated frequencies are in good agreement with the measured spectrum. According to the calculations, the higher frequency band corresponds to the free OH stretch of the terminal  $\text{H}_2\text{O}$  molecule in the trimer. The lower frequency band comes from the excitation of the free OH stretch of the central  $\text{H}_2\text{O}$  molecule, which serves as an acceptor from HCl and a donor to the second  $\text{H}_2\text{O}$  molecule. It is seen that calculations are not reproducing the relative intensity of the two bands.

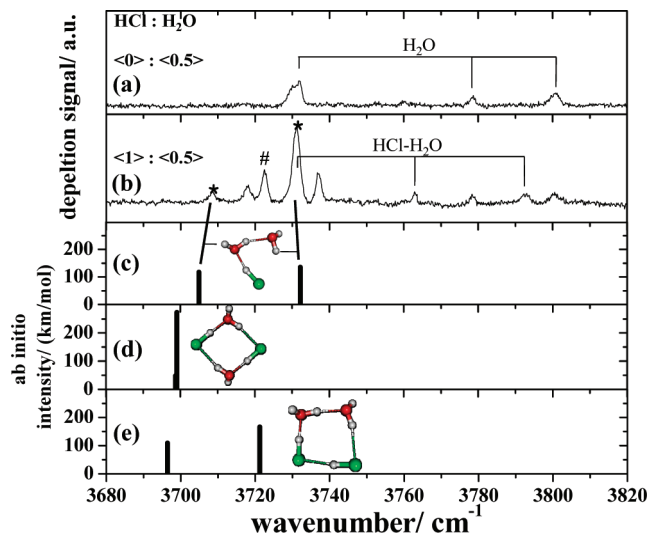


**Figure 6.** Comparison of the spectra measured at  $\langle N_{\text{water}} \rangle = 0.5$  (a) and  $\langle N_{\text{HCl}} \rangle : \langle N_{\text{water}} \rangle = 1:0.5$  (b). The bands asterisked originate from clusters having one HCl and several water molecules. The below panels show the calculated spectra of the pseudocyclic  $\text{HCl}(\text{H}_2\text{O})_2$  (c) and  $(\text{HCl})_2(\text{H}_2\text{O})_2$  (d and e) clusters to aid the assignment of the  $\text{HCl}(\text{H}_2\text{O})_2$  complex. The calculated frequencies are scaled by a factor of 0.957.

The band of the  $\text{HCl}(\text{H}_2\text{O})_2$  clusters at  $3731\text{ cm}^{-1}$  has a close overlap with the asymmetric stretch of the acceptor molecule in water dimers at  $3730\text{ cm}^{-1}$ . Therefore, these bands cannot be resolved. However, in Figure 6, it is seen that the FWHM of the combined band becomes smaller when the  $\text{HCl}(\text{H}_2\text{O})_n$  clusters are formed, which is also seen in Figures 2, 4, and S1. On the other hand, the intensity of the band with respect to the  $\text{H}_2\text{O}$  and the  $\text{HCl}-\text{H}_2\text{O}$  lines increases with  $\langle N_{\text{HCl}} \rangle$ . These transformations indicate that at  $\langle 1 \rangle : \langle 0.5 \rangle$  in Figure 6b, the band at  $3731\text{ cm}^{-1}$  predominantly comes from the  $\text{HCl}(\text{H}_2\text{O})_2$  clusters. Good correspondence of the calculated and measured frequencies suggests the pseudocyclic planar structure of the  $\text{HCl}(\text{H}_2\text{O})_2$  clusters in agreement with previous studies.<sup>36</sup> Poisson distribution shows that about one-third of the band's intensity may come from the two conformers of  $(\text{HCl})_2(\text{H}_2\text{O})_2$  clusters whose bar spectra are shown in panels (d) and (e). The energies of these two different conformers are very similar to each other as shown in Figure S4 in the Supporting Information. However, their frequency assignments are beyond the scope of the present study.

**4.4.  $\text{HCl}(\text{H}_2\text{O})_3$  Clusters.** Figure 7 shows the comparison of the spectrum (a) of neat water clusters at  $\langle N_{\text{water}} \rangle = 2$  with spectrum (b) measured at  $\langle N_{\text{HCl}} \rangle = 1$  and  $\langle N_{\text{water}} \rangle = 2$ . Panels (c) and (d) show the calculated spectra for the cyclic and T-shaped  $\text{HCl}(\text{H}_2\text{O})_3$  clusters, respectively.

Ab initio calculations show that the global minimum structure for  $\text{HCl}(\text{H}_2\text{O})_3$  is cyclic, which resembles that of the cyclic water tetramer. The structural similarities between the  $(\text{H}_2\text{O})_4$  and  $\text{HCl}(\text{H}_2\text{O})_3$  clusters (both cyclic) suggest that they may have similar spectra. However, the perturbation due to the replacement of a water molecule by HCl induces the splitting of the free OH stretches as shown in the bar spectrum in Figure 7c. The splitting pattern appears to be similar to that observed in the measured spectrum shown in Figure 7b.

On the other hand, the higher energy (15.4 kJ/mol) T-shaped isomer has two closely spaced lines in Figure 7d, whose pattern is not observed in the measured spectrum. Therefore, we concluded that the  $\text{HCl}(\text{H}_2\text{O})_3$  clusters are cyclic, corresponding to the global minimum. Observation of the cyclic structure of the  $\text{HCl}(\text{H}_2\text{O})_3$  clusters implies that the third  $\text{H}_2\text{O}$  molecule is able to insert into the preformed pseudocyclic  $\text{HCl}(\text{H}_2\text{O})_2$

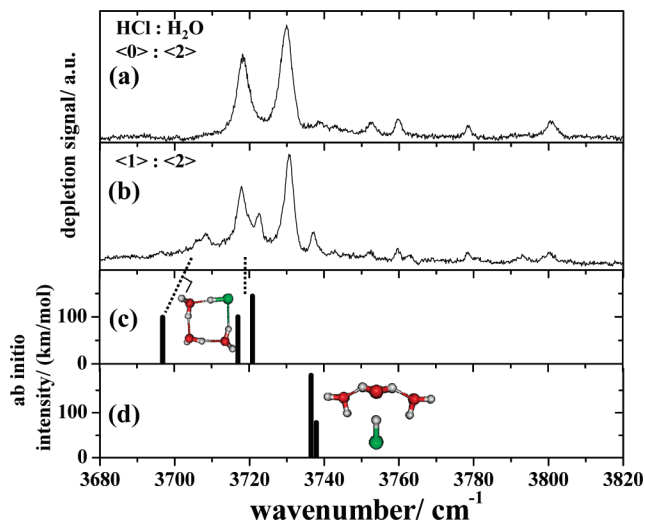


**Figure 7.** Spectrum of clusters obtained at  $\langle N_{\text{water}} \rangle = 2$  (a) and at  $\langle N_{\text{HCl}} \rangle : \langle N_{\text{water}} \rangle = 1:2$  (b). Panels (c) and (d) show the calculated spectra of the  $\text{HCl}(\text{H}_2\text{O})_3$  clusters having cyclic and T-shaped configurations, respectively. The dotted lines show the tentative assignments of the bands. Calculated frequencies are scaled by a factor of 0.957.

clusters. Insertion of water molecules into ring clusters up to pentamers has been observed previously in neat  $(\text{H}_2\text{O})_n$ <sup>41</sup> and  $(\text{HCl})_n$  clusters.<sup>33</sup>

## 5. Conclusions

In this study of the  $(\text{HCl})_m(\text{H}_2\text{O})_n$  clusters, we have identified the clusters of one HCl with up to three water molecules and two HCl with one water molecule in the free OH stretching spectral range of  $3680\text{--}3820\text{ cm}^{-1}$ . The congestion of the bands of the larger clusters in the region of  $3700\text{--}3740\text{ cm}^{-1}$  makes the assignments of the clusters having more than three water molecules difficult. In the spectrum of the  $\text{HCl}-\text{H}_2\text{O}$  dimer, a nearly prolate symmetric top, the rotational constant  $A$  of  $14.85\text{ cm}^{-1}$  was deduced very similar to that obtained in the gas phase. The analysis of the spectra suggests that  $\text{HCl}(\text{H}_2\text{O})_2$  and  $\text{HCl}(\text{H}_2\text{O})_3$  clusters formed in He droplets are cyclic, in agreement with the results of ab initio calculations. Spectra of the  $\text{HCl}(\text{H}_2\text{O})_n$  clusters in the bonded O-H and H-Cl stretch regions will be presented in the near future.

**Acknowledgment.** This material is based upon work supported by NSF grant CHE 0513163 and the Korea Research Foundation Grant funded by the Korean Government (MOEHRD, Basic Research Promotion Fund) (KRF-313-C00339). Calculations were performed using the supercomputing resources of the Korean Institute of Science and Technology Information (KISTI) and the Korean Science and Engineering Foundation (KOSEF) grant funded by the Korea government (MEST) (No. R01-2008-000-20002-0(2008)). We are grateful to Luis Gomez for careful reading of this manuscript.

**Supporting Information Available:** (i) Spectra of  $(\text{HCl})_m(\text{H}_2\text{O})_n$  clusters measured at small abundance of HCl and  $\text{H}_2\text{O}$  in the droplets. (ii) Survey spectra in the free OH region of the neat water clusters obtained at different abundance of  $\text{H}_2\text{O}$  molecules. (iii) Structures and relative energies of the two conformers of  $(\text{HCl})_2(\text{H}_2\text{O})_2$ . This material is available free of charge via the Internet at <http://pubs.acs.org>.

## References and Notes

- (1) Packer, M. J.; Clary, D. C. *J. Phys. Chem.* **1995**, *99*, 14323.

- (2) Re, S.; Osamura, Y.; Suzuki, Y.; Schaefer, H. F. *J. Chem. Phys.* **1998**, *109*, 973.
- (3) Bacelo, D. E.; Binning, R. C.; Ishikawa, Y. *J. Phys. Chem. A* **1999**, *103*, 4631.
- (4) Sobolewski, A. L.; Domcke, W. *J. Phys. Chem. A* **2003**, *107*, 1557.
- (5) Sobolewski, A. L.; Domcke, W. *Phys. Chem. Chem. Phys.* **2005**, *7*, 970.
- (6) Svanberg, M.; Pettersson, J. B. C.; Bolton, K. *J. Phys. Chem. A* **2000**, *104*, 5787.
- (7) Buch, V.; Sadlej, J.; Aytemiz-Uras, N.; Devlin, J. P. *J. Phys. Chem. A* **2002**, *106*, 9374.
- (8) Bacelo, D. E.; Fioressi, S. E. *J. Chem. Phys.* **2003**, *119*, 11695.
- (9) Chaban, G. M.; Gerber, R. B.; Janda, K. C. *J. Phys. Chem. A* **2001**, *105*, 8323.
- (10) Devlin, J. P.; Uras, N.; Sadlej, J.; Buch, V. *Nature (London)* **2002**, *417*, 269.
- (11) Ando, K.; Hynes, J. T. *J. Mol. Liq.* **1995**, *64*, 25.
- (12) Ault, B. S.; Pimentel, G. C. *J. Phys. Chem.* **1973**, *77*, 57.
- (13) Schriver, A.; Silvi, B.; Maillard, D.; Perchard, J. P. *J. Phys. Chem.* **1977**, *81*, 2095.
- (14) Amirand, C.; Maillard, D. *J. Mol. Struct.* **1988**, *176*, 181.
- (15) Andrews, L.; Wang, X. F.; Mielke, Z. *J. Phys. Chem. A* **2001**, *105*, 6054.
- (16) Andrews, L.; Wang, X. F.; Mielke, Z. *J. Am. Chem. Soc.* **2001**, *123*, 1499.
- (17) Devlin, J. P.; Farnik, M.; Suhm, M. A.; Buch, V. *J. Phys. Chem. A* **2005**, *109*, 955.
- (18) Delzeit, L.; Rowland, B.; Devlin, J. P. *J. Phys. Chem.* **1993**, *97*, 10312.
- (19) Uras, N.; Rahman, M.; Devlin, J. P. *J. Phys. Chem. B* **1998**, *102*, 9375.
- (20) Weimann, M.; Farnik, M.; Suhm, M. A. *Phys. Chem. Chem. Phys.* **2002**, *4*, 3933.
- (21) Farnik, M.; Weimann, M.; Suhm, M. A. *J. Chem. Phys.* **2003**, *118*, 10120.
- (22) Huneycutt, A. J.; Stickland, R. J.; Hellberg, F.; Saykally, R. J. *J. Chem. Phys.* **2003**, *118*, 1221.
- (23) Hurley, S. M.; Dermota, T. E.; Hydutsky, D. P.; Castleman, A. W. *Science* **2002**, *298*, 202.
- (24) Hurley, S. M.; Dermota, T. E.; Hydutsky, D. P.; Castleman, A. W. *J. Chem. Phys.* **2003**, *118*, 9272.
- (25) Callegari, C.; Lehmann, K. K.; Schmied, R.; Scoles, G. *J. Chem. Phys.* **2001**, *115*, 10090.
- (26) Toennies, J. P.; Vilesov, A. F. *Angew. Chem., Int. Ed.* **2004**, *43*, 2622.
- (27) Choi, M. Y.; Douberly, G. E.; Falconer, T. M.; Lewis, W. K.; Lindsay, C. M.; Merritt, J. M.; Stiles, P. L.; Miller, R. E. *Int. Rev. Phys. Chem.* **2006**, *25*, 15.
- (28) Stienkemeier, F.; Lehmann, K. K. *J. Phys. B: At. Mol. Opt. Phys.* **2006**, *39*, R127.
- (29) Hartmann, M.; Miller, R. E.; Toennies, J. P.; Vilesov, A. *Phys. Rev. Lett.* **1995**, *75*, 1566.
- (30) Hartmann, M.; Miller, R. E.; Toennies, J. P.; Vilesov, A. F. *Science* **1996**, *272*, 1631.
- (31) Frisch, M. J.; Trucks, G. W.; Schlegel, H. B.; Scuseria, G. E.; Robb, M. A.; Cheeseman, J. R.; Montgomery, J. A., Jr.; Vreven, T.; Kudin, K. N.; Burant, J. C.; Millam, J. M.; Iyengar, S. S.; Tomasi, J.; Barone, V.; Mennucci, B.; Cossi, M.; Scalmani, G.; Rega, N.; Petersson, G. A.; Nakatsuji, H.; Hada, M.; Ehara, M.; Toyota, K.; Fukuda, R.; Hasegawa, J.; Ishida, M.; Nakajima, T.; Honda, Y.; Kitao, O.; Nakai, H.; Klene, M.; Li, X.; Knox, J. E.; Hratchian, H. P.; Cross, J. B.; Adamo, C.; Jaramillo, J.; Gomperts, R.; Stratmann, R. E.; Yazyev, O.; Austin, A. J.; Cammi, R.; Pomelli, C.; Ochterski, J. W.; Ayala, P. Y.; Morokuma, K.; Voth, G. A.; Salvador, P.; Dannenberg, J. J.; Zakrzewski, V. G.; Dapprich, S.; Daniels, A. D.; Strain, M. C.; Farkas, O.; Malick, D. K.; Rabuck, A. D.; Raghavachari, K.; Foresman, J. B.; Ortiz, J. V.; Cui, Q.; Baboul, A. G.; Clifford, S.; Cioslowski, J.; Stefanov, B. B.; Liu, G.; Liashenko, A.; Piskorz, P.; Komaromi, I.; Martin, R. L.; Fox, D. J.; Keith, T.; Al-Laham, M. A.; Peng, C. Y.; Nanayakkara, A.; Challacombe, M.; Gill, P. M. W.; Johnson, B.; Chen, W.; Wong, M. W.; Gonzalez, C.; Pople, J. A. *Gaussian 03*, revision C.02; Gaussian, Inc.: Wallingford, CT, 2004.
- (32) Slipchenko, M.; Kuyanov, K.; Sartakov, B.; Vilesov, A. F. *J. Chem. Phys.* **2006**, *124*, 241101.
- (33) Skvortsov, D.; Choi, M. Y.; Vilesov, A. F. *J. Phys. Chem. A* **2007**, *111*, 12711.
- (34) Lewerenz, M.; Schilling, B.; Toennies, J. P. *J. Chem. Phys.* **1995**, *102*, 8191.
- (35) Kuyanov, K. E.; Slipchenko, M. N.; Vilesov, A. F. *Chem. Phys. Lett.* **2006**, *427*, 5.
- (36) Kisiel, Z.; Pietrewicz, B. A.; Fowler, P. W.; Legon, A. C.; Steiner, E. *J. Phys. Chem. A* **2000**, *104*, 6970.
- (37) Legon, A. C.; Willoughby, L. C. *Chem. Phys. Lett.* **1983**, *95*, 449.
- (38) Ayers, G. P.; Pullin, A. D. E. *Spectrochim. Acta* **1976**, *32A*, 1695.
- (39) Kisiel, Z.; Bialkowska-Jaworska, E.; Pszczolkowski, L.; Milet, A.; Struniewicz, C.; Moszynski, R.; Sadlej, J. *J. Chem. Phys.* **2000**, *112*, 5767.
- (40) Skvortsov, D.; Lee, S. J.; Choi, M. Y.; Vilesov, A. F., in preparation.
- (41) Nauta, K.; Miller, R. E. *Science* **2000**, *287*, 293.